

## 2 Å X-ray structure of adamalysin II complexed with a peptide phosphonate inhibitor adopting a retro-binding mode

M. Cirilli<sup>a</sup>, C. Gallina<sup>b</sup>, E. Gavuzzo<sup>a</sup>, C. Giordano<sup>b</sup>, F.X. Gomis-Rüth<sup>c</sup>, B. Gorini<sup>b</sup>,  
L.F. Kress<sup>d</sup>, F. Mazza<sup>a,\*</sup>, M. Paglialunga Paradisi<sup>b</sup>, G. Pochetti<sup>a</sup>, V. Politi<sup>e</sup>

<sup>a</sup>Ist. Strutturistica Chimica, CNR, C.P. n. 10, 00016 Monterotondo Stazione, Rome, Italy

<sup>b</sup>Centro Chimica del Farmaco, CNR, Università 'La Sapienza', 00185 Rome, Italy

<sup>c</sup>Dpt. de Biologia Molecular i Cellular, Centre d'Investigació i Desenvolupament C.S.I.C., Jordi Girona, 18-26, 08034 Barcelona, Spain

<sup>d</sup>Molecular and Cellular Biology Dpt., Roswell Park Cancer Institute, Buffalo, NY 14263, USA

<sup>e</sup>Polifarma Research Center, V. Tor Sapienza 138, 00155 Rome, Italy

Received 18 September 1997; revised version received 20 October 1997

**Abstract** The search of reprotolysin inhibitors offers the possibility of intervention against both matrixins and ADAMs. Here we report the crystal structure of the complex between adamalysin II, a member of the reprotolysin family, and a phosphonate inhibitor modeled on an endogenous venom tripeptide. The inhibitor occupies the primed region of the cleavage site adopting a retro-binding mode. The phosphonate group ligates the zinc ion in an asymmetric bidentate mode and the adjacent Trp indole system partly fills the primary specificity subsite S<sub>1</sub>'. An adamalysin-based model of tumor necrosis factor- $\alpha$ -converting enzyme (TACE) reveals a smaller S<sub>1</sub>' pocket for this enzyme.

© 1997 Federation of European Biochemical Societies.

**Key words:** X-ray crystal structure; Zinc-endopeptidase; Snake venom proteinase; Phosphonate inhibitor; Tumor necrosis factor- $\alpha$ -converting enzyme

### 1. Introduction

Reprotolysins, also known as adamalysins [1], are snake venom zinc-endopeptidases that hydrolyze basement membrane proteins involved in the adhesion among capillary endothelial cells, inducing extensive haemorrhages in the bitten preys [2]. Matrixins (matrix metalloproteinases, MMPs) are zinc-dependent enzymes that degrade the major components of the extracellular matrix. Although they play an important physiological role in tissue remodeling and repair, their aberrant regulation has been implicated in pathologies such as tumor metastasis, rheumatoid arthritis and multiple sclerosis [3]. These two classes of proteinases, together with serralytins and astacins, have been grouped into the superfamily of 'met-zincins' [1], because of similar zinc-dependent catalytic domains. The similarities of reprotolysins and MMPs [4], as well as their high degree of tertiary structure conservation at the active site [5], suggest that the binding of substrates and inhibitors may be similar. Depending on the number of domains, the multimodular reprotolysins have been subdivided in four classes: P-I, when only a zinc-dependent proteolytic domain is contained, P-II, P-III and P-IV, when a disintegrin, a cysteine-rich and a lectin domain, respectively are also included [6]. Interestingly, also animal tissues produce a large number of multi-domain proteins, generally called ADAMs [7], that contain the same domains of P-IV reprotolysins, and

have been therefore included in this family of enzymes [8]. ADAMs are present in a wide range of organisms and mammalian tissues and appear to be transmembrane proteins whose physiological role has not yet been clearly understood, even though some of them seem involved in fertilization processes [9], neurogenesis [10] or degradation of bovine myelin basic protein [11]. The tumor necrosis factor- $\alpha$  (TNF- $\alpha$ ) is a cytokine involved in many inflammatory diseases [12] and is released into blood circulation by TNF- $\alpha$ -converting enzyme (TACE). According to a recent finding TACE belongs to the group of ADAM 10 [13].

In this context, the search of reprotolysin inhibitors offers the possibility of intervention against both matrixins and ADAMs. Moreover, the finding that in crotalid and viperid snake venoms there are also present large amounts of pyroglutamate (Pyr) containing tripeptides (Pyr-Asn-Trp and Pyr-Glu-Trp), acting as weak and competitive inhibitors of reprotolysins [14], suggested us to modify these endogenous peptides rather than the natural substrates, for obtaining novel types of more powerful inhibitors. Tripeptide derivatives such as Pyr-Leu-Trp-OMe (POL509) and 2-Furoyl-Leu-Trp (POL647) have been already tested as possible innovative agents in the field of immunological reactions and for reducing damages induced by snake venoms and TNF- $\alpha$ . At this regard, POL509 showed immunomodulatory effects in rats 'in vivo' [15], depending on increased antigen presentation efficiency [16]; POL647 inhibited the haemorrhagic activity of *Echis Pyramidum Laekeyi* venom and its isolated haemorrhagin [17] and prevented the processing of TNF- $\alpha$  precursor by snake venom reprotolysins [18]. Further modifications of the above peptides, promoting tighter binding to the adamalysin II active site, considered as the reprotolysin prototype [19], have been carried out by our group. Novel compounds, characterized by the presence of a phosphonate group and possessing broad spectrum inhibitory activities on some zinc-dependent proteinases have been synthesized and will be reported in a forthcoming paper. In order to reveal the mode of binding of these phosphonate inhibitors, here we report the crystal structure of adamalysin II complexed with an analogue of POL647, in which the terminal carboxyl has been replaced by the phosphonate group.

### 2. Materials and methods

For preparation of the inhibitor the diastereomeric diethyl esters 2-Furoyl-Leu-(D,L)Trp(P)(OEt)<sub>2</sub> were synthesized and separated by silica-gel chromatography. The corresponding phosphonic acids

\*Corresponding author. Fax: +39 (6) 90672630.  
E-mail: mazza@isc.mlib.cnr.it

were obtained by hydrolysis. The phosphonic acid deriving from the fast-moving (TLC) diethyl ester gave an  $IC_{50} = 0.3 \mu M$  on adamalysin II, a value about ten times smaller than that showed by the other diastereomer. The more potent isomer was used for preparation of the complex. The configuration at the Trp(P)  $C^\alpha$  was determined by the present investigation and is reported in Section 3.

Adamalysin II was purified as previously described [20].

Crystals of the complex were obtained by sitting drop vapour diffusion technique. Droplets were made by mixing 6  $\mu l$  of a 5 mg/ml adamalysin II solution in 5 mM  $CaCl_2$ , 5 mM  $ZnCl_2$ , 1 mg/ml inhibitor, 10 mM Tris, pH 8, with 1.5  $\mu l$  of a 1.8 M  $(NH_4)_2SO_4$  solution, pH 5. Droplets were allowed to equilibrate against the same  $(NH_4)_2SO_4$  buffer as reservoir solution at 4°C. Trigonal, prism shaped crystals of maximum dimension 0.5 mm  $\times$  0.2 mm  $\times$  0.1 mm were obtained and harvested with 2.5 M  $(NH_4)_2SO_4$  solution, 5 mM  $CaCl_2$ , 5 mM  $ZnCl_2$ , 2 mM inhibitor, pH 5.

X-ray intensity data were collected at 4°C on a 180 mm MAR image plate area detector (MAR Research, Hamburg) with the Synchrotron Radiation Source at Elettra (Trieste), processed by DENZO [21] and CCP4 [22]. Native protein coordinates were taken from the PDB (ref. 1IAG) [23]. Refinement was performed by XPLOR [24]. Molecular modeling of the inhibitor was made by Chem-X [25], electron density maps were inspected using O [26] on a Silicon Graphics workstation. Data collection and refinement statistics are reported in Table 1. The coordinates of the inhibitor complex have been deposited with the PDB (ref. 4AIG).

The inhibitory activity was measured by the fluorescence of the cleaved substrate 2-aminobenzoyl-Ala-Gly-Leu-Ala-p-nitrobenzylamide at different inhibitor concentrations.

### 3. Results and discussion

The structure of the complexed enzyme is practically identical to that of the native enzyme [19]. The root-mean-square deviation between the backbone atoms of the inhibited and native enzyme is 0.26 Å. The largest deviations affect the  $C^\alpha$  atoms of the Pro<sup>168</sup>-Leu<sup>170</sup> segment that is exposed to the solvent. The active site is characterized by the strictly conserved zinc-binding motif HExxHxxGxxH. The 'edge strand' Ile<sup>108</sup>-Ser<sup>114</sup> together with the segment His<sup>129</sup>-Leu<sup>135</sup> form the 'upper rim' of the active site cleft while the segment Pro<sup>168</sup>-Leu<sup>170</sup> separates the  $S_1'$  pocket from the bulk solvent. These segments furnish groups for the binding of either the substrate or the inhibitor.

The 'omit' electron density map, shown in Fig. 1, clearly fits the stereoisomer corresponding to the (R)-Trp(P), therefore the inhibitor is the *N*-[(furan-2-yl)carbonyl]-(S)-leucyl-(R)-[1-amino-2(1*H*-indol-3-yl)ethyl]-phosphonic acid. This map also shows that the inhibitor peptide chain occupies the primed region of the cleavage site, adopting an almost extended conformation; the largest deviation from the extended form is given by the Leu residue with  $\varphi = -83^\circ$ ,  $\psi = 133^\circ$ .



Fig. 1. Stereo view of the adamalysin II active site and inhibitor superimposed on the final  $2F_o - F_c$  electron density map contoured at  $1\sigma$ .

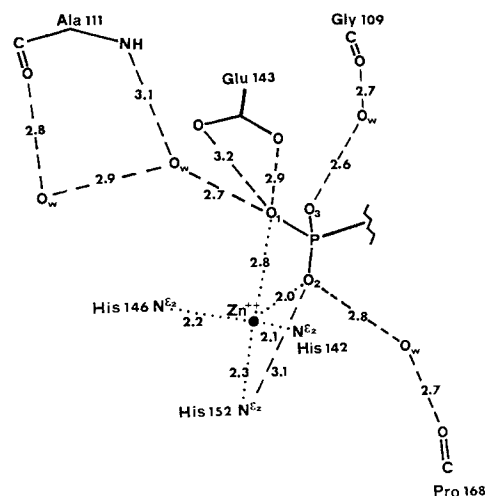


Fig. 2. Schematic representation of the interactions formed by the phosphonate group in the active site. Dotted and dashed lines represent zinc coordination and possible H-bonds, respectively. Distances in Å.

Two phosphonate oxygens ligate the electrophilic zinc ion in an asymmetric bidentate mode (distances are 2.0 and 2.8 Å, respectively) as shown in Fig. 2, provoking displacement of the catalytically essential water molecule that in the uncomplexed enzyme is the fourth zinc ligand [19]. Similar asymmetric bidentate binding mode between zinc ion and oxygen atoms bound to phosphorous containing inhibitors have been found in the crystal structures of complexes of thermolysin [27,28], carboxypeptidase A [29] and astacin [30].

The zinc ion adopts a distorted tetrahedral geometry; among the coordination angles, the His<sup>152</sup>  $N^{\epsilon_2}$ -Zn-O<sub>1</sub> ( $145^\circ$ ) presents the largest deviation. The distorted coordination allows the approach to the metal of the additional phosphonic oxygen O<sub>1</sub> (2.8 Å) that is also close to both oxygens (2.9 and 3.2 Å) of the Glu<sup>143</sup> side-chain. This residue is sup-

Table 1  
Data collection and refinement statistics

Crystal system	Trigonal
Space group	P3 <sub>2</sub> 12
Cell parameters (Å)	a = b = 73.5, c = 96.9
$\lambda$ (Å)	1.0
No. collected data	53112
No. unique reflections	19533
Completeness (%) (all shells)	95.4 (20.0–2.0 Å)
Completeness (%) (last shell)	98.3 (2.05–2.00 Å)
$R_{merge}$	0.112
Resolution range	20.0–2.0 Å
No. reflections used in refinement	18583
Protein atoms (all active)	1607
Water molecules	191
R-factor	0.177 (6.0–2.0 Å)
Mean B factor (Å <sup>2</sup> ) - protein	22.2
Mean B factor (Å <sup>2</sup> ) - inhibitor	29.7
Mean B factor (Å <sup>2</sup> ) - ions	16.5
Mean B factor (Å <sup>2</sup> ) - waters	42.2
R.m.s. deviation (Å) - bonds	0.007
R.m.s. deviation (°) - angles	0.95

$R_{merge} = \sum_h \sum_i (|I(h,i) - \langle I(h) \rangle|) / \sum_h \sum_i I(h,i)$ , where  $I(h,i)$  is the intensity value of the  $i$ th measurement of  $h$  and  $\langle I(h) \rangle$  is the corresponding mean value of  $h$  for all  $i$  measurements of  $h$ .

R-factor =  $\sum |F_o - F_c| / \sum F_o$ .

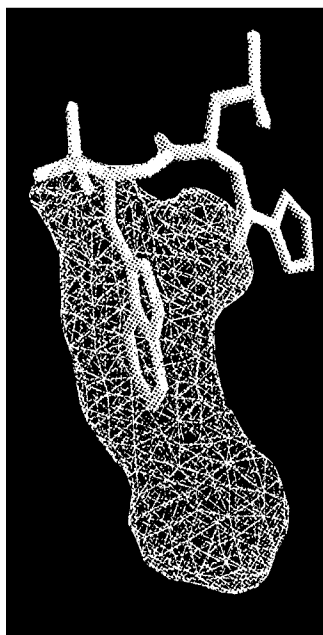


Fig. 3. Shape of the  $S_1'$  pocket partly filled by the Trp side-chain of the inhibitor, drawn by GRASP [32].

posed to polarize the zinc bound water molecule for the nucleophilic attack to the scissile peptide bond during enzyme hydrolysis [31].

The inhibitor Trp indole ring, adopting the ( $g^+$ , $t$ ) conformation, occupies the unusually deep primary specificity  $S_1'$  subsite, with an orientation almost parallel to the ring of His<sup>142</sup> and a distance between the two ring centroids of 3.4 Å. Moreover, the Trp side-chain N<sup>H</sup> is anchored to the Arg<sup>167</sup> CO group by a H-bond. It is interesting to observe that the bulky side-chain of Trp has replaced three water molecules that are present in the  $S_1'$  pocket of the native enzyme [19]; this suggests that the internal water molecules can be displaced and ejected into bulk solvent. However, the  $S_1'$  pocket is not completely filled by the Trp side-chain and its lower part still contains two ordered water molecules interconnected by H-bonds with themselves and the surrounding polar groups (Cys<sup>164</sup> CO, Ile<sup>165</sup> CO, Gly<sup>169</sup> CO, Thr<sup>171</sup> NH). These solvent positions furnish useful indications for the design of bulkier groups to insert at P<sub>1</sub>' position of the inhibitor for enhancing its binding affinity. We have calculated the volumes

Table 2

Structure-based sequence alignment of adamalysin II (ADA) and TACE reported around the edge strand segment of the 'upper rim' (residues 102–114), the zinc-binding consensus sequence (residues 130–154) and the Met-turn (residues 165–170)

	102		114
ADA	. . . N F E G K I I G K A Y T S . . .		
TACE	. . . D F D M G T L G L A Y V G . . .		
	130		154
ADA	. . . S P I N L L V A V T M A H E L G H N L G M E H D G . .		
TACE	. . . T I L T K E A D L V T T H E L G H N F G A E H D P . .		
	165		170
ADA	. . . I M R P G L . . .		
TACE	. . . V M Y P I A . . .		

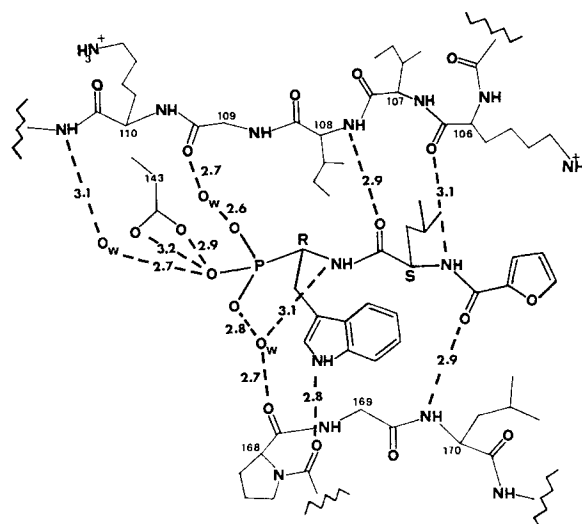


Fig. 4. Scheme of the H-bonds (dashed lines, distances in Å) between the active site and inhibitor polar groups. The letters R and S indicate the configurations at the chiral centers of the inhibitor.

of the adamalysin II  $S_1'$  pocket (306 Å<sup>3</sup>) and of its portion not filled by the inhibitor (189 Å<sup>3</sup>) using the program GRASP [32]. These values are comparable with those found for the complex between Ht-d and Pyr-Asn-Trp [33] and indicate that the  $S_1'$  pocket is not even half filled by the Trp side-chain (see Fig. 3). A progressive decrease of the  $S_1'$  pocket volume has been found in the human neutrophil collagenase [34] and human fibroblast collagenase [35].

The network of H-bonds between the inhibitor and the active site polar groups is shown in Fig. 4. Interestingly, the inhibitor backbone adopts a retro-binding mode, with its chain direction parallel to the  $\beta$ -sheet segment Ile<sup>108</sup>-Ser<sup>114</sup> of the 'upper rim' and antiparallel to the cross over and  $S_1'$  wall forming segment Pro<sup>168</sup>-Leu<sup>170</sup>. Although the direction is reversed to that generally adopted by all substrate-based inhibitors of MMPs [36], its backbone forms H-bonds with the same groups of the catalytic core, except for the Trp NH that is H-bonded to a water molecule. A similar amino to carboxyl direction has been found for the extended portion of the pro-domain in the active site of stromelysin-1 [37].

The inhibitor Leu side-chain adopts the  $g^-(t, g^-)$  conformation and one of its methyl groups forms van der Waals contacts of 3.2 and 3.8 Å with the Gly<sup>105</sup> CO and one methyl group of Ile<sup>107</sup>, respectively. The furan ring is loosely involved in interactions with the surrounding groups.

A structure-based sequence alignment of adamalysin II and TACE [12], partly reported in Table 2, was performed using the program MODELLER [38]. The inspection of the modeled TACE active site reveals substantial similarities to those of adamalysin II, particularly for the elongated zinc-binding consensus sequence, the Met-turn, and the edge strand segment Lys<sup>106</sup>-Ala<sup>111</sup> of the 'upper rim'. However, the most notable difference is the smaller  $S_1'$  pocket of TACE, due to the presence of a Leu residue in place of adamalysin II Val<sup>138</sup>.

#### 4. Conclusion

Because of potential toxicity associated with the extensively used hydroxamate inhibitors of MMPs and their preclusion to

bind both S and S' regions of the active site, other ligands are being exploited. The crystal structure of adamalysin II complexed with a phosphonate inhibitor modeled on an endogenous venom tripeptide, reveals that the terminal phosphonate group ligates the zinc ion in an asymmetric bidentate mode. The inhibitor backbone occupies the primed region, adopting a retro-binding mode, with the amino to carboxyl chain direction opposite to that normally adopted by the substrate-based inhibitors. This finding can suggest new ideas for the design of novel specific inhibitors against adamalysin II and related enzymes. Finally, a structural model of TACE reveals a S<sub>1</sub>' pocket smaller than that of adamalysin II.

**Acknowledgements:** We thank Prof. W. Bode (Max-Planck-Institut, Martinsried) for encouraging this work, Drs. L. Barba and V. Fares for helpful suggestions. This project was supported by a grant from CNR (Progetto Strategico).

## References

- [1] Bode, W., Gomis-Rüth, F.X. and Stöcker, W. (1993) *FEBS Lett.* 331, 134–140.
- [2] Bjarnason, J.B. and Fox, J.W. (1995) in: *Methods in Enzymology* (Barrett, A.J., Ed.) vol. 248, pp. 345–368, Academic Press, San Diego, CA.
- [3] Woessner Jr., J.F. (1994) *Ann. N.Y. Acad. Sci.* 732, 11–21.
- [4] Jiang, W. and Bond, J.S. (1992) *FEBS Lett.* 312, 110–114.
- [5] Stöcker, W., Grams, F., Baumann, U., Reinemer, P., Gomis-Rüth, F.X., McKay, D.B. and Bode, W. (1995) *Protein Sci.* 4, 823–840.
- [6] Bjarnason, J.B. and Fox, J.W. (1994) *Pharmacotherapy* 62, 325–372.
- [7] Wolfsberg, T.G., Straight, P.D., Gerena, R.L., Huovila, A.-P.J., Primakoff, P., Myles, D.G. and White, J.M. (1995) *Dev. Biol.* 169, 378–383.
- [8] Rawlings, N.D. and Barrett, A.J. (1995) in: *Methods in Enzymology* (Barrett, A.J., Ed.) vol. 248, pp. 183–228, Academic Press, San Diego, CA.
- [9] Blobel, C.P., Myles, D.G., Primakoff, P. and White, J.M. (1990) *J. Cell Biol.* 111, 69–78.
- [10] Rooke, J., Pan, D., Xu, T. and Rubin, G.M. (1996) *Science* 273, 1227–1230.
- [11] Howard, L. and Glynn, P. (1995) in: *Methods in Enzymology* (Barrett, A.J., Ed.) vol. 248, pp. 388–395, Academic Press, San Diego, CA.
- [12] Moss, M.L., Jin, S.-L.C., Milla, M.E., Burkhart, W., Carter, H.L., Chen, W.-J., Clay, W.C., Didsbury, J.R., Hassler, D., Hoffman, C.R., Kost, T.A., Lambert, M.H., Leesnitzer, M.A., McCauley, P., McGeehan, G., Mitchell, J., Moyer, M., Pahel, G., Rocque, W., Overton, L.K., Schoenen, F., Seaton, T., Su, J.-L., Warner, J., Willard, D. and Becherer, J.D. (1997) *Nature* 385, 733–736.
- [13] Lunn, C.A., Fan, X., Dalie, B., Miller, K., Zavodny, P.J., Nair, S.K. and Lundell, D. (1997) *FEBS Lett.* 400, 333–335.
- [14] Robeva, A., Politi, V., Shannon, J.D., Bjarnason, J.B. and Fox, J.W. (1991) *Biomed. Biochim. Acta* 50, 769–773.
- [15] Mattei, M., Gorini, A., Lavaggi, M.V., Sumerska, T., Politi, V. and Colizzi, V. (1991) *J. Chemother.* 3, 160–164.
- [16] Gilardini-Montani, M.S., Tuosto, L., Delfini, M., Gueritore, D., Starace, G., Politi, V. and Piccolella, E. (1993) *Immunopharmacology* 25, 51–63.
- [17] Laing, G.D. and Politi, V. (1995) *Toxicon* 33, 261.
- [18] Moura-da-Silva, A.M., Laing, G.D., Paine, M.J.I., Dennison, J.M.T.J., Politi, V., Crampton, J.M. and Theakston, R.D.G. (1996) *Eur. J. Immunol.* 26, 2000–2005.
- [19] Gomis-Rüth, F.X., Kress, L.F., Kellermann, J., Mayr, I., Lee, X., Huber, R. and Bode, W. (1994) *J. Mol. Biol.* 239, 513–544.
- [20] Kurecki, T., Laskowski, M.S. and Kress, F. (1978) *J. Biol. Chem.* 253, 8340–8345.
- [21] Otwinowski, Z. and Minor, W. (1996) in: *Methods in Enzymology* (Carter Jr., C.W. and Sweet, R.M., Eds.) vol. 276, Academic Press, San Diego, CA.
- [22] Collaborative Computational Project, Number 4 (1994) *Acta Cryst. D50*, 760–763.
- [23] Bernstein, F.C., Koetzle, T.F., Williams, G.J.B., Meyer Jr., E.F., Brice, M.D., Rodgers, J.R., Kennard, O., Shimanouchi, T. and Tasumi, M. (1977) *J. Mol. Biol.* 112, 535–542.
- [24] Brünger, A.T. (1992) *X-PLOR Manual Version 3.1*, Yale University, New Haven, CT.
- [25] Chem-X (1988) Chemical Design Ltd., Oxford.
- [26] Jones, T.A., Zou, J.-Y., Cowan, S.W. and Kjeldgaard, M. (1991) *Acta Cryst. A47*, 110–119.
- [27] Tronrud, D.E., Monzingo, A.F. and Matthews, B.W. (1986) *Eur. J. Biochem.* 157, 261–268.
- [28] Holden, H.M., Tronrud, D.E., Monzingo, A.F., Weaver, L.H. and Matthews, B.W. (1987) *Biochemistry* 26, 8542–8553.
- [29] Kim, H. and Lipscomb, W.N. (1990) *Biochemistry* 29, 5546–5555.
- [30] Grams, F., Dive, V., Yiotakis, A., Yiallouris, I., Vassiliou, S., Zwilling, R., Bode, W. and Stocker, W. (1996) *Nature Struct. Biol.* 3, 671–675.
- [31] Matthews, B.W. (1988) *Acc. Chem. Res.* 21, 333–340.
- [32] Nicholls, A., Sharp, K.A. and Honig, B. (1991) *Proteins Struct. Funct. Genet.* 11, 281–296.
- [33] Botos, I., Scapozza, L., Zhang, D., Liotta, L.A. and Meyer, E.F. (1996) *Proc. Natl. Acad. Sci. USA* 93, 2749–2754.
- [34] Grams, F., Crimmin, M., Hinnes, L., Huxley, P., Pieper, M., Tschesche, H. and Bode, W. (1995) *Biochemistry* 34, 14012–14020.
- [35] Stams, T., Spurlino, J.C., Smith, D.L., Wahl, R.C., Ho, T.F., Qoronfle, M.W., Banks, T.M. and Rubin, B. (1994) *Struct. Biol.* 1, 119–123.
- [36] Grams, F., Reinemer, P., Powers, J.C., Kleine, T., Pieper, M., Tschesche, H., Huber, R. and Bode, W. (1995) *Eur. J. Biochem.* 228, 830–841.
- [37] Becker, J.W., Marcy, A.I., Rokosz, L.L., Axel, M.G., Burbaum, J.J., Fitzgerald, P.M.D., Cameron, P.M., Esser, C.K., Hagmann, W.K., Hermes, J.D. and Springer, J.P. (1995) *Protein Sci.* 4, 1966–1976.
- [38] Sali, A. and Blundell, T.L. (1993) *J. Mol. Biol.* 234, 779–815.